Studies of Magnetic Properties of Fine Particles
and their Relevance to Materials Science
J.L. Dormann and D. Fiorani (Editors)

Preparation of Fine Particles

G. C. Hadjipanayis[a], Z. X. Tang[b], S. Gangopadhyay[a], L. Yiping[a], C. M. Sorensen[b], K. J. Klabunde[b], A. Kostikas[c], and V. Papaefthymiou[d]

[a]Department of Physics & Astronomy, University of Delaware, Newark, DE 19716, USA

[b]Departments of Physics & Chemistry, Kansas State University, Manhattan, KS 66506, USA

[c]National Research Center Demokritos, Aghia Paraskevi, Athens, Greece.

[d]Department of Physics, University of Ioannina, Ioannina, Greece.

Abstract

The techniques of vapor deposition, aerosol spray pyrolysis and chemical reduction have been used to prepare fine magnetic particles. Fe particles were prepared with an average size in the range of 50-300 Å by varying the gas pressure during evaporation (1-30 torr). Fe-B particles have been produced by chemical reduction with $NaBH_4$. The size (100-500 Å) and the boron concentration of the particles were varied by changing the reduction conditions. Amorphous and crystallized barium ferrite particles with a size of about 1000 Å have been synthesized from metal salts by an aerosol technique. The magnetic and structural properties of all these particles were studied with SQUID magnetometry and transmission electron microscopy, respectively. The magnetic properties of the ultrafine metallic particles can be explained by a particle morphology consisting of an oxide shell around a metallic core.

1. INTRODUCTION

Fine particles exhibit properties which are drastically different from the bulk. This opens up an area of research that is very challenging scientifically and technologically. Fine particles have been widely used for magnetic recording media, ferro-fluids, catalysts, medical diagnostics, drug delivery systems and pigments in paints and ceramics [1-3]. Enhanced magnetic properties of fine ferromagnetic or ferrimagnetic particles make them very promising candidates for high density magnetic recording media. A large number of techniques have been used to prepare magnetic fine particles including chemical reduction [4], hydrothermal [5], sputtering [6], SMAD (solvated metallic atom deposition) [7], gas evaporation [8] and aerosol synthesis.

Evaporated fine Fe particles (~ 200 Å) have been reported to have coercivities up to

two orders of magnitude higher than bulk Fe and their saturation magnetization varied from 20 - 90 % of the bulk value depending on particle size [9]. Particles in their fine form (few 100's of Å) are pyrophoric and hence require a controlled surface passivation. The magnetic properties of the particles are strongly dependent on the form and constituents of the surface layers which constitute a major volume fraction in ultra-fine particles. Thus a greater understanding and control of the surface layer would result in optimum magnetic properties.

After Schlesinger et al [10] reported that transition metal-boron powders can be produced by chemical reduction in aqueous solution, a number of studies have dealt with the magnetic and structural properties of these fine particles [11-14]. The systems we have studied include Fe-B, Fe-Ni-B, Fe-Co-B, and Co-B particles. The magnetic properties of fine particles prepared by chemical reduction have also been found to be different from the bulk. The results on Fe-B particles are discussed below.

Aerosols, which are particles dispersed in a gas, are used in agriculture, forestry, industry and medicine [15]. Scientists also use the aerosol processes to prepare metal oxides, and ceramics [16-18]. In our aerosol synthesis, often called aerosol spray pyrolysis, aqueous metal salts were sprayed as a fine mist, dried and then passed into a hot flow tube where pyrolysis converted the salts to the final products.

In this paper, we will briefly summarize our efforts in the last three years to prepare fine magnetic particles using the techniques of vapor deposition, chemical reduction and aerosol spray pyrolysis.

2. EXPERIMENTAL METHODS

2.1. Vapor deposition

In the vapor deposition technique, the particle size can be effectively controlled by varying several parameters including the molecular weight of the inert gas, evaporation source temperature, inert gas pressure and the substrate temperature. In our experiment, an alumina-coated tungsten crucible was used to evaporate the metal. The distance between the crucible and the water cooled Cu substrate was optimized in order to maximize the yield. Argon gas was used to provide the inert atmosphere during evaporation. The dynamic pressure of argon used during evaporation varied between 1 and 30 torr. The metal particles made by this technique are highly pyrophoric and require surface passivation which, as it will be shown later, plays an important role in determining the magnetic behavior of the whole particle. An argon-air mixture was introduced into the chamber for this purpose after evaporation (the volume ratio of argon to O_2 being about 300).

2.2. Chemical reduction

Transition metal-boron powders were prepared by reducing aqueous solutions of metal salts with $NaBH_4$. The composition and structure of the powders were found to depend on the method of sample preparation. Amorphous high boron content powders with boron content as high as 40 at% are usually produced by adding the $NaBH_4$ solution into a well stirred iron salt solution, However, if the two solutions are slowly mixed in a "Y-junction", a low boron content powder is obtained which is found to be crystalline. The

maximum amount of boron that was found in the Fe-B powders was 15 at% when the "Y-junction" technique was used. The particle size could be varied by changing the solvent and concentration of the solution. The black precipitates were separated and repeatedly washed with distilled water and acetone, and then dried in an Ar atmosphere chamber.

2.3. Aerosol spray pyrolysis

The apparatus for the aerosol synthesis of fine particles was described elsewhere [19]. To make barium iron oxide particles, $Fe(NO_3)_3{\cdot}9H_2O$ and $Ba(NO_3)_2$ were dissolved in distilled deionized water with Fe/Ba atomic ratio of 12. The concentration of the precusor solution was varied from 0.2 to 20 wt%. The solution was nebulized by a constant output atomizer at a N_2 pressure of 35 *psi*. The liquid drop aerosol stream passed through a diffusion dryer to remove the water. The dried salt particles then passed through a quartz tube which was held at 800 °C. The residence time of the particles in this tube was about 1.4 seconds. The aerosol particles were collected on cover glasses by thermophoresis at the end of the furnace tube. Powder samples were obtained by scraping the particles off the cover glasses. Once the particles were obtained, further heat treatments, beyond the few seconds of residence time in the high temperature tube, were made in a nitrogen environment at different temperatures. The aerosol technique has two main advantages in synthesizing fine particles. First, materials are mixed in solution hence they are homogeneously mixed at the start on the atomic level. Second, only low temperatures are necessary to form crystallized particles.

3. STRUCTURAL AND MAGNETIC PROPERTIES

3.1 Vapor Deposition

The particles obtained by this technique have a particle size in the range of 50-300 Å. The particle diameter was found to increase as the gas pressure increased. With increasing gas pressure the mean free path of the metal vapors is decreased, because of more collisions, leading to the formation of larger particles.

Structural and morphological analysis of the particles were performed using X-ray diffraction, selected area electron diffraction (SAD) and transmission electron microscopy (TEM). Samples were found to contain bcc α-Fe, Fe_3O_4 and γ-Fe_2O_3. The oxide lines were always broad and diffuse due to their polycrystalline form [20]. As shown by TEM, the particles were roughly spherical, with a ring contrast, which could be due to a shell/core type of structure, where the shell consists of

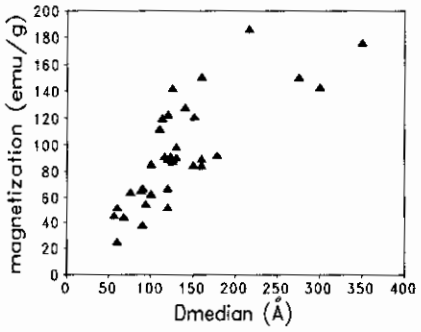

Figure 1. Size dependence of saturation magnetization in Fe particles.

Fe-oxides and the core of metallic Fe [21]. The particle size was found to follow a log-normal distribution. Small particles were more uniform in their size distribution as compared to the bigger particles.

The magnetic properties were found to be strongly dependent on particle size. As the

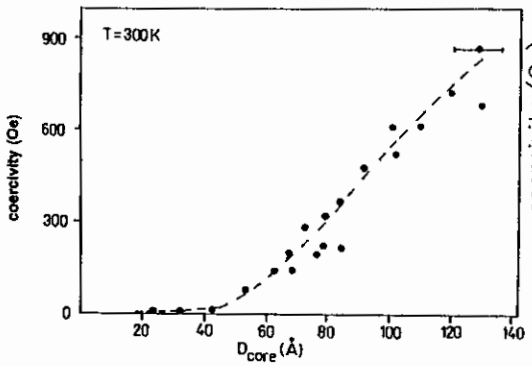

Figure 2. Size dependence of coercivity for Fe particles at room temperature. Particles with core diameter below 40 Å show superparamagnetism.

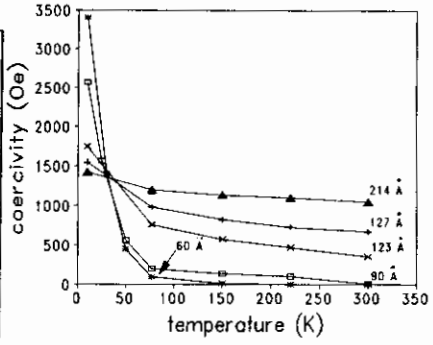

Figure 3. Temperature dependence of coercivity for Fe particles of different sizes. Note the crossover temperature of curves at about 30 - 40 K.

size increased from 60 to 200 Å, the magnetization values increased from 25 to 190 emu/g, which are 11.4% and 86.4% of the bulk Fe magnetization, respectively. This behavior is shown in figure 1. The decrease in magnetization with decreasing particle size is due to the increased volume fraction of the oxide because of the higher surface to volume ratio in the smaller particles. Furthermore, as the particle size decreases finite size effects play a stronger role, resulting in the pinning of the surface moments which leads to a lower magnetization [22,23].

The room temperature coercivity decreases as the particle size decreases, as shown in figure 2 (due to thermal effects [24]). The maximum value of coercivity obtained at room temperature was 1140 Oe for a sample with a particle size of 214 Å. The coercivity showed a very strong temperature dependence in smaller particle samples as compared to the bigger ones (figure 3). The particles with a total diameter below 70 Å were found to be superparamagnetic below room temperature. Note the sharp increase in coercivity below 40 K in all the samples. Below this temperature the size dependence of coercivity is reversed, as compared to that at room temperature.

3.2. Chemical reduction

X-ray diffraction patterns showed that when the boron content in Fe-B is higher than 20 at%, the powders were amorphous; otherwise they were crystalline with a bcc structure. TEM micrographs (figure 4) show that particles form chains with a width of

300- 600 Å. Figure 5 shows the magnetization and coercivity as a function of boron concentration. M_s is found to decrease initially with B content, going through a minimum at 15 at% and then increase again for higher B content. The largest change in magnetization was observed in the smallest particles. The coercivity displayed the opposite behavior with a maximum value of about 1000 Oe at 15 at% B.The large difference between the values of M_s for the smaller and larger particles can be explained by the surface oxidation effect as we discussed in section 3.1. When the B content is higher than 20 at%, the particles become amorphous and they do not oxidize as much as in the crystalline state leading to higher

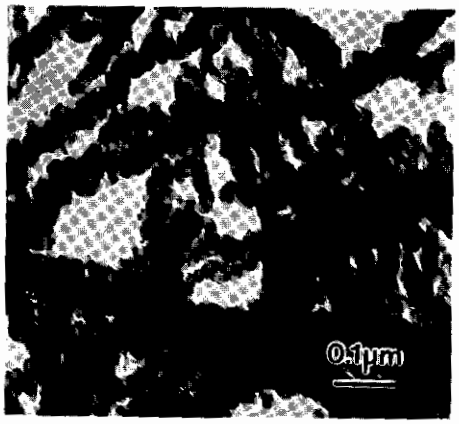

Figure 4. Micrograph of Fe-B particles.

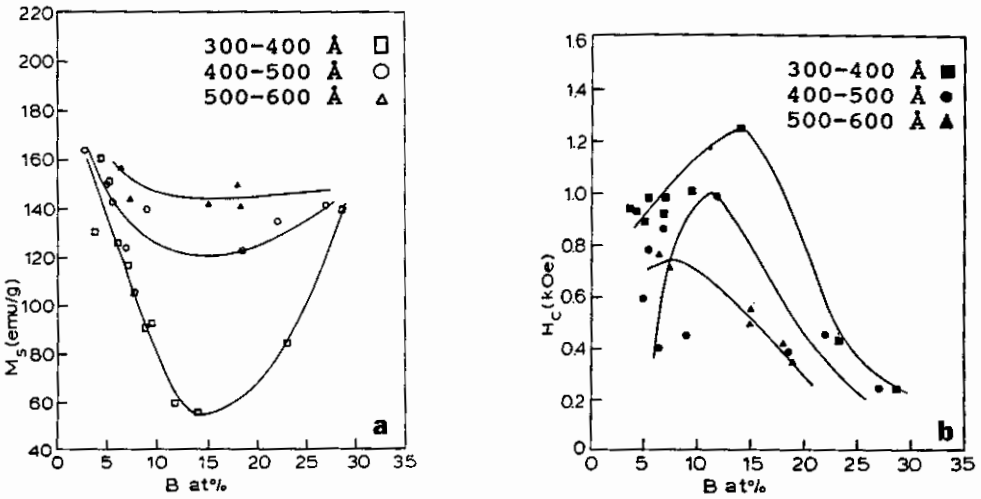

Figure 5. (a) Magnetization and (b) coercivity as functions of B content in Fe-B particles at 10 K.

M_s. Also, this oxidized layer enhances the total magnetic anisotropy and leads to a large H_c.

Typical Mössbauer spectra obtained for the amorphous and crystalline samples are

shown in figure 6. The spectrum of the amorphous sample consists clearly of a magnetic hyperfine pattern and a paramagnetic one. The component with broad lines and an effective hyperfine field near 273 kG belongs to amorphous Fe-B. The quadroupole doublet at 85 K becomes magnetic at 4.2 K with an average hyperfine field 485 kG. The spectrum of the crystalline sample can be analyzed as a superposition of three magnetic hyperfine patterns as shown by the solid line. The first component with narrow lines and an effective field of 340 kG is easily recognized as α-Fe. The other two component have broad lines and an average hyperfine field 490 kG. This hyperfine field is similer to that observed in amorphous Fe-B samples at cryogenic temperatures and is attributed to γ-Fe_2O_3 particles [25].

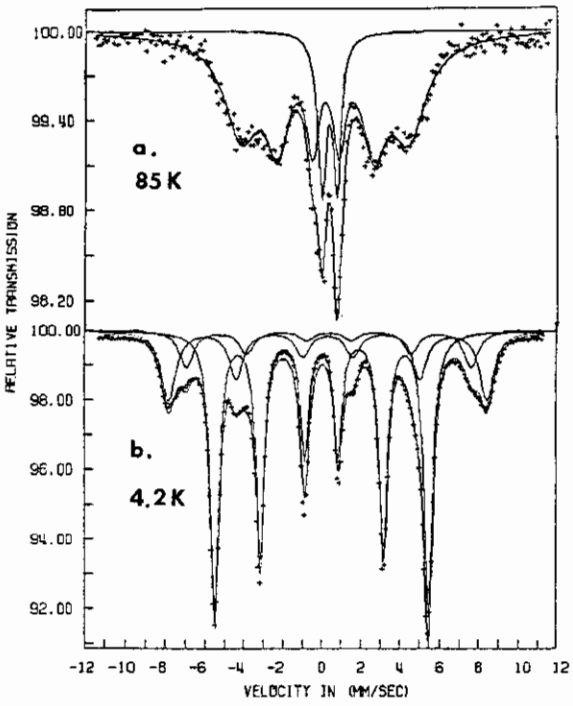

Figure 6. Mössbauer spectra for Fe-B particles (a) amorphous, (b) crystalline.

The Mössbauer data are consistent with the "shell/core" type particle morphology observed in the Fe particles. An indirect experiment supported the presence of an oxide coating around the Fe-B core. A sample was prepared by drying the as-made powder in a N_2 atmosphere inside a chamber. The sample was then split into two halves; the first was packed in a sample holder outside the chamber and the other one inside the chamber. The two samples were found to have different coercivities, 900 and 750 Oe, with the higher value obtained on the sample packed outside the chamber. Thus it may be speculated that the coercivity of the sample is mainly due to the surface oxide layers which coat the Fe-B core.

3.3 Aerosol spray pyrolysis

For the as-received Ba-Fe ferrite sample from the precusor solution of 2 wt%, the x-ray diffraction showed an amorphous phase but with the atomic ratio of Fe to Ba as in the stoichiometric barium ferrite (Fe/Ba=12). The amorphous characteristics of the as-received sample from aerosol synthesis is the result of our aerosol preparation technique. Iron and barium nitrate molecules were randomly distributed in the aqueous

solution. This random structure remained in the particles even after the diffusion dryer removed H_2O and the furnace tube decomposed the iron nitrate and barium nitrate mixture to a phase in the form of barium iron oxide. The 1.4 s residence time, however, was not long enough to crystallize the amorphous state. The decomposition temperature must be crucial for the creation of this amorphous state. Lower temperatures may not be able to decompose iron nitrate and barium nitrate similateneously, while higher temperatures may cause crystallization. This arguement was supported by Kaczmarek *et al* [26] who obtained multiple oxide phases at a deposition temperature of 527 °C and a single crystallized ferrite phase at a deposition temperature of 1027 °C using similar synthesis procedures. Residence time may also have the equivalent effects.

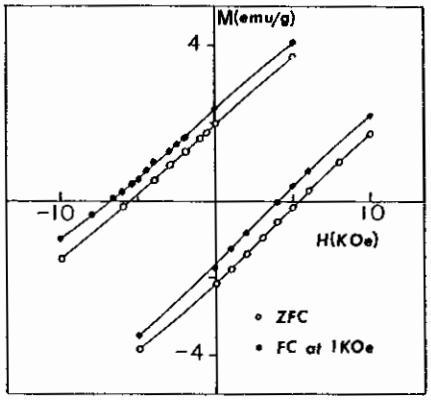

Figure 7. Central part of the hysteresis loops for as-received barium Ba-Fe ferrite particles.

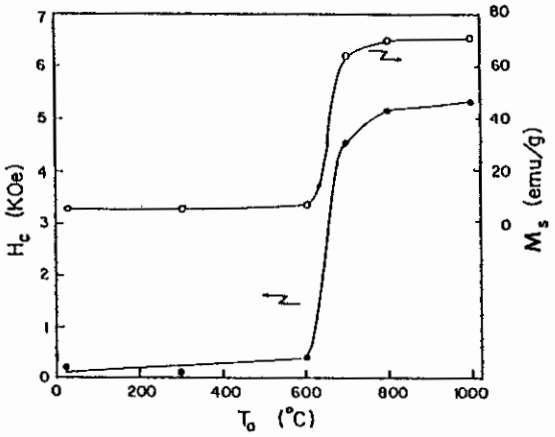

Figure 8. Saturation magnetization and coercivity of aerosol barium ferrite particles as a function of annealing temperature (T_a) in a N_2 atmosphere.

We measured the temperature dependence of magnetization which exhibited a maximum near 180 *K* when the sample was zero-field cooled (ZFC) and then measured in a field of 400 *Oe*. This maximum was almost flattened with field cooling (FC) in 400 *Oe* and it totally disappeared in samples field cooled in 10^4 *Oe* [27]. We also measured the hysteresis loop below the maximum temperature (T_f). Figure 7 shows only the central part of the two hysteresis loops measured on FC and ZFC samples. The zero field cooled loop is symmetric about H=0 while the FC loop (1 *kOe)* is shifted to the negative field side. The shifted loop has its center at H=-1350 *Oe* with the isothermal remanent magnetization being less than the

thermoremanent magnetization. These features are characteristic of a spin glass behavior [28].

The amorphous state of the as-received sample was confirmed by DSC measurements which showed an exothermic peak indicating the onset of crystallization at 687 °C with a 20 °C/min heating rate. Heat-treating the as-received samples in a nitrogen environment resulted in changes of both the microstructure and particle morphology. The as-received sample had a broad distribution of spherical particles with an average diameter of 800 Å. Heat treatment changed these spherical particles to platelet-shaped particles which are typical for barium ferrite. These platelet-shaped particles had an average thickness of 400 Å with an aspect ratio of 3.5:1. X-ray diffraction studies showed clearly a single barium ferrite phase in samples heat-treated at 800 °C. Magnetic properties revealed a simple transition from the amorphous state to the crystallized state. Figure 8 shows the saturation magnetization (M_s) and coercivity (H_c) at room temperature as a function of annealing temperature (T_a) (the annealing time was 1 hour). No change was detected below 600 °C for the saturation magnetization. Samples experienced a dramatical change in saturation magnetization between 600 and 800 °C. These results are in good agreement with the DSC results. A sample annealed at 1000 °C reached a saturation magnetization of 70.6 emu/g which was very close to the bulk value (72 emu/g). The highest coercivity (5360 *Oe*) was obtained by annealing at about 1000 °C.

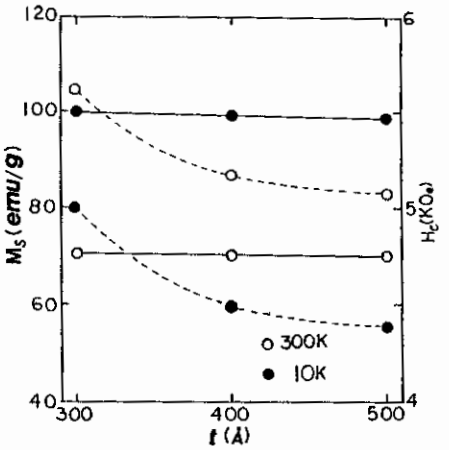

Figure 9. Size dependence of saturation magnetization (solid lines) and coercivity (dashed lines) in aerosol synthesized barium ferrite particles.

In the aerosol technique, particle size can be changed by changing the salt concentration in the precursor solution, because the volume of the final solid particle is proportional to the concentration of the precusor solution. We used three concentrations, 0.2, 2 and 20 wt%, and obtained three samples with different particle size. After a heat-treatment at 800 °C for 1 hour in N_2, the particles had different thickness with the aspect ratios unchanged (3.5:1). M_s and H_c of these three samples are as shown in figure 9. Particle size does not affect the saturation magnetization but does affect the coercivity. When the average particle size decreases, more particles become single domain, and this leads to a larger coercivity [29].

4. THE "SHELL-CORE" MODEL

The structural, magnetic and Mössbauer data indicate a shell/core type of particle morphology in the Fe and Fe-B particles. In Fe particles, the core consists of metallic α-Fe, and the shell is composed of its oxides (Fe_3O_4/γ-Fe_2O_3). In the Fe-B particles the core is an amorphous Fe-B matrix in the amorphous sample (B > 20 at%) and bcc Fe(B) in the crystalline samples. The shell consists of Fe_3O_4/γ-Fe_2O_3. The shell/core model can explain adequately the magnetic hysteresis behavior and the size dependence of magnetization in these particles.

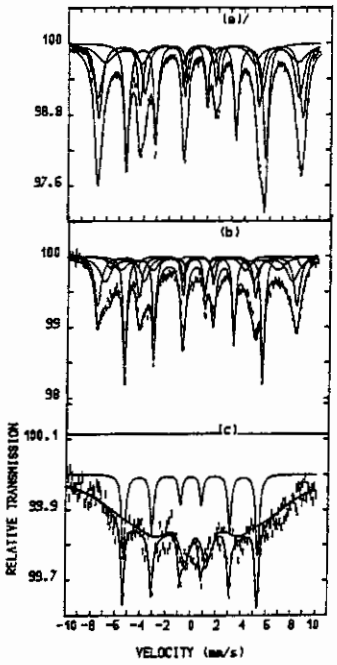

Figure 10. Mössbauer spectra of a 114 Å sized Fe sample at: (a) 4.2 K (b) 85 K (c) 300 K

From the Mössbauer spectra of Fe particles (shown in figure 10) [30], it was evident that both the Fe and Fe-oxides are ferromagnetic below 85 K, (the sharp sextet corresponding to α-Fe). However, above 85 K the oxide becomes superparamagnetic and because of the interaction with the ferromagnetic Fe ("core") [20], a broad doublet is observed superimposed on the α-Fe sextet. From $H_c(T)$ curves (figure 3, measured with SQUID) the superparamagnetic transition temperature of the oxide coating was predicted to be between 30 - 40 K (about one third than that predicted by Mössbauer spectroscopy, due to different measurement times of the two techniques). The exchange interaction between the ferromagnetic Fe core and the Fe-oxide shell results in the enhancement of coercivity values at lower temperatures (< 40 K). Above the blocking temperature (~ 40 K) of the oxide coating ("shell"), the coercivity of the whole particle decreases very sharply, because of the small size of the Fe-core and its interaction with the superparamagnetic oxide shell.

This model was further strengthened by the behavior of Fe/Ag samples where the amount of oxide on the particle surface was minimized by covering the particles with a thin film of Ag before exposing the sample to the ambient [31]. This resulted in a strong reduction of the temperature dependence of coercivity (as expected); furthermore, the crossover among the coercivity vs temperature curves disappeared, as it is shown in figure 11.

In Fe-B the size of the particles is much larger than the size of the Fe particles (by

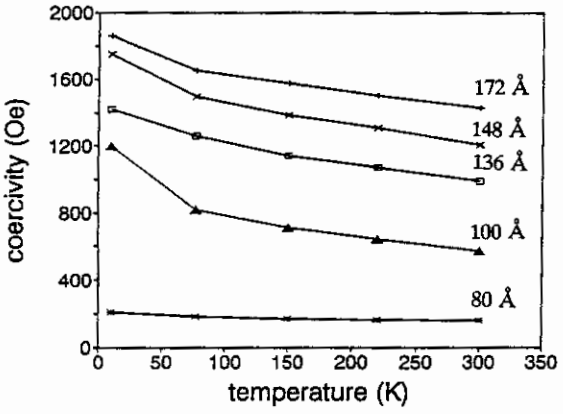

Figure 11. Reduced temperature dependence of coercivity in the case of Fe/Ag samples; the crossover temperature is not present as in the case of passivated Fe samples.

approximately a factor of 5) and therefore the effect of shell/core interface exchange interaction is not strong enough to affect the magnetic behavior of the particle as a whole. This results in a normal $H_c(T)$ behavior with a small increase in coercivity with decreasing temperature down to the blocking temperature of the Fe-oxide where a stronger $H_c(T)$ dependence is observed.

As it was pointed out earlier, the magnetization is usually decreased with decreasing particle size, because of dilution effects due to the lower magnetization of the oxides. However, the magnetization values below 90 emu/g can not be explained by the dilution hypothesis. In the past a similar effect was observed in fine Fe-oxide particles, where magnetization values as small as 30 emu/g were observed in γ-Fe_2O_3 [32]. The reduced magnetization values have been attributed to different effects. Berkowitz et al [32] explained the lower M_s by assuming the existence of a non-magnetic layer ("dead" layer) at the surface of the particles. Later Morrish et al [33] and Coey et al [22] claimed that the "dead" layer is due to surface spin canting. Recently this hypothesis has been disputed, however, and Pankhurst [23] claimed that the lower magnetization values are due to non-saturation (of magnetization) effects because of the random distribution of the small Fe-oxide particles with enhanced values of magnetocrystalline anisotropy. Research in this area is presently very active and the latest results suggest that the low M_s values are due to bulk spin-canting in the whole particle [34].

5. CONCLUSIONS

Fe particles in the size of 50-300 Å have been obtained by vapor deposition with a maximum coercivity of 1200 Oe. Iron ions can be easily reduced by $NaBH_4$ to form iron borides. The particle size and boron concentration in the final products can be varied by changing the reduction conditions. Coercivities as high as 1300 Oe have been obtained. Amorphous barium ferrite fine particles with magnetic properties characteristic of spin glass have been prepared by the aerosol technique. The magnetic properties of annealed samples showed a dramatic change from the amorphous to the crystallized state. Coercivity of the crystallized $BaFe_{12}O_{19}$ increases with decreasing particle size while saturation magnetization is nearly independent of particle size.

The structural and magnetic data for the finer particles of Fe and Fe-B are very

similar. The magnetization and coercivity dependence on size and temperature could be explained using a shell/core model, which induces an exchange anisotropy at the shell/core interface resulting in an enhancement of coercivity at 10 K.

6. ACKNOWLEDGMENTS

This work has been supported by NSF CHE-9013930. We also acknowledge the support of a Nato Research Grant for Dr. Hadjipanayis.

REFERENCES

1 E. Matijević, MRS Bulletin XIV (1989) 19.
2 M. Ozaki, MRS Bulletin XIV (1989) 35.
3 M.P. Sharrock and R.E. Bodnar, J. Appl. Phys. 57 (1989) 3919.
4 T. Miyahara and K. Wawakauri, IEEE Trans. Magn. MAG-23 (1987) 2877.
5 S. Komarneni, E. Fregeau, E. Breval, and R. Roy, J. Am. Ceram. Soc. 71(1) (1988) C-26.
6 G. Xiao and C.L. Chien, J. Appl. Phys. 61 (1987) 3308.
7 C.F. Kernizan, K.H. Klabunde, C.M. Sorensen, and G.C. Hadjipanayis, J. Appl. Phys. 67(9) (1990) 5897.
8 C. Hayashi, J. Vac. Sci. Tech. A5 (1987) 1375.
9 A. Tasaki, M. Takao, and H. Tokunaga, Japn. J. Appl. Phys. 13 (1974) 27.
10 H.I. Schlesinger, H.C. Brown, J. Am. Chem. Soc. 75 (1953) 215.
11 S.G. Kim, J.R. Brock, J. Coll. Interf. Sci. 116 (1987) 431.
12 S. Nafis, G.C. Hadjipanayis, C.M. Sorensen, and K.J. Klabunde, IEEE. Trans. Magn. Mag-25 (1989) 3641.
13 L. Yiping, G.C. Hadjipanayis, C.M. Sorensen, and K.J. Klabunde, J. Magn. Magn. Mater. 79 (1989) 321.
14 S. Linderoth, S. Morup, A. Meagher, J. Larsen, and M.D. Bentzon, J. Magn. Magn. Mater. 81 (1989) 138.
15 W.C. Hinds, *Aerosol Technology* (John Wiley & Sons, New York, 1982).
16 M. Gani and R. McPhreson, J. Mater. Sci. **15** (1989) 1915.
17 K. Kumar, A. Petrovich, C. Williams, and J. Van der Sande, J. Appl. Phys. **64** (1988) 5665.
18 T.T. Kodas, E.M. Engler, and V.Y. Lee, Appl. Phys. Lett. **54** (1989) 1923.
19 Z.X. Tang, S. Nafis, C.M. Sorensen, G.C. Hadjipanayis, and K.J.Klabunde, IEEE Trans. Magn. 25 (1989) 4236.
20 K. Haneda and A. H. Morrish, Surf. Sci. **77** (1978) 584.
21 S. Gangopadhyay and G. C. Hadjipanayis, Submitted to Phys. Rev. B.
22 J. M. D. Coey, Phys. Rev. Lett., **27** (1972) 1140.
23 Q. A. Pankhurst and R. J. Pollard, Phys. Rev. Lett. **67** (1991) 248.
24 E. F. Kneller and F. E. Luberosky, J. Appl. Phys. **34** (1963) 656.
25 A.M Van Der Kraan, Phys. Stat. Sol.(a) 1s. (1973) 2156.
26 W.A. Kaczmarek, B.W. Ninham, and A. Calka, The 5th Joint MMM-Intermag

Conference (Pittsburgh, 1991).
27 Z.X. Tang, S. Nafis, C.M. Sorensen, G.C. Hadjipanayis, and K.J. Klabunde, J. Magn. Magn. Mater. **80** (1989) 285.
28 K. Moorjani and J.M.D. Coey, Magnetic Glasses (Elsevier, New York, 1984) p.36.
29 G.C. Hadjipanayis, E. Singleton, and Z.X. Tang, J. Magn. Magn. Mater. **81** (1989)
30 V. Papaefthymiou, A. Kostikas, A. Simopoulos, D. Niarchos, S. Gangopadhyay, G. C. Hadjipanayis, C. M. Sorensen, and K. J. Klabunde, J. Appl. Phys. **67**(9) (1990) 4487.318.
31 S. Gangopadhyay, G.C. Hadjipanayis, S.I. Shah, C.M. Sorensen, K.J. Klabunde, V. Papaefthymiou, and A. Kostikas, J. Appl. Pys. 70 (1991)
32 A.E. Berkowitz, W.J. Schuele, and P.J. Flanders, J. Appl. Phys. 39 (1968) 1261.
33 A.H. Morrish, K. Haneda, and P.J. Schurer, J. Phys. Colloq. 37 (1976) C6-301.
34 F.T. Parker, M.W. Foster, D. Margulies, and A.E. Berkowitz, J. Appl. Phys. 68(8) (1991) 4505.